

# Deformation of Amorphous GeSe<sub>2</sub> Film under Uniaxial Pressure Applied at Elevated Temperatures

Byeong Kyou Jin, Jun Ho Lee, Jeong Han Yi, Woo Hyung Lee, Sang Yeol Shin,  
and Yong Gyu Choi<sup>†</sup>

*Department of Materials Science and Engineering, Korea Aerospace University, Gyeonggi 412-791, Republic of Korea*

(Received January 12, 2015; Revised February 5, 2015; Accepted February 11, 2015)

## ABSTRACT

In an effort to evaluate the practicability of an imprinting technique for amorphous chalcogenide film in Ge-based compositions, we investigate the deformation behavior of the surface of amorphous GeSe<sub>2</sub> film deposited via a thermal evaporation route according to varying static loads applied at elevated temperatures. We observe that, under these static loading conditions, crystallization tends to occur on its surface relatively more easily than in As-based As<sub>2</sub>Se<sub>3</sub> films. As for the present GeSe<sub>2</sub> film, higher processing temperatures are required in order to make its surface reflect the given stamp patterns well; however, in this case, its surface becomes partially crystallized in the monoclinic GeSe<sub>2</sub> phase. The increased vulnerability of this amorphous GeSe<sub>2</sub> film toward surface crystallization under static loading, when compared with the As<sub>2</sub>Se<sub>3</sub> counterpart, is explained in terms of the topological aspects of its amorphous structure.

**Key words :** Chalcogenide glass, Amorphous Ge-Se film, Imprinting, Surface crystallization

## 1. Introduction

The imprinting (or embossing) technique that can introduce functionally useful patterns on the surface of bulk or film chalcogenide glass is considered to be a viable option that can be applied to fabricating electronic or photonic devices based on chalcogenide glass. This non-oxide glass typically exhibits significantly lower glass transition temperatures compared with conventional oxide glasses. In general, among the numerous chalcogenide glass forming systems, those glasses that contain As and/or Ge are more thermally stable, and thus attract significantly more attention in numerous practical applications. It should be noted that the As-based glasses have been predominantly utilized in verifying the feasibility of imprinting technique; Seddon *et al.* investigated the fundamental characteristics of the morphological evolution of the surface during the imprinting process.<sup>1-4)</sup> Solmaz *et al.* attempted to accommodate an active agent in order to improve the quality of the imprinted surface of the As<sub>2</sub>S<sub>3</sub> film.<sup>5)</sup> More recently, Madden *et al.* were successful in demonstrating the fabrication of a rib waveguide of arsenic selenide glass with the propagation loss limited by the Rayleigh scattering.<sup>6)</sup> Based on these previous experimental results, it might be considered that the imprinting technique of these As-based chalcogenide glasses is promising, even though more efforts are required in order to

implement the imprinted structures during device fabrication procedures. In addition to the As-based glasses (stoichiometric As<sub>2</sub>S<sub>3</sub> or As<sub>2</sub>Se<sub>3</sub> compositions in particular) as a candidate material for the imprinting technique, Ge-based glasses should be available.

Compared with these As-based chalcogenide glasses, however, there are few studies that have been conducted using Ge-based glasses. Therefore, in this study, we investigated the deformation behavior of amorphous Ge-Se film under uniaxial pressure applied at elevated temperatures in an effort to empirically establish its thermo-mechanical characteristics. In particular, the evaporation-deposited Ge-Se film with a composition of Ge<sub>33</sub>Se<sub>67</sub> in atomic percent was selected, and its surface deformed under various experimental circumstances was monitored, which was then compared with As-based glasses. A tendency toward the surface crystallization observed in the present GeSe<sub>2</sub> film is explained in connection with the processing conditions and its amorphous structure.

## 2. Experimental Procedure

As starting materials, germanium (Ge) and selenium (Se) with purities of 99.999% were used in their elemental form to fabricate 'bulk' glass via the conventional melt-quenching route. As stated above, the compositional ratio used in this study was Ge<sub>33</sub>Se<sub>67</sub> (at%). After being carefully weighed, each batch was vacuum-sealed inside a silica ampoule and then melted at 1000°C for 24 h using a rocking furnace. Quenching was conducted through immersing the ampoule into ice water, and annealing was subsequently undertaken

<sup>†</sup>Corresponding author : Yong Gyu Choi  
E-mail : ygchoi@kau.ac.kr  
Tel : +82-2-300-0169 Fax : +82-2-3158-3779

at a temperature below its glass transition temperature for 1 h in a vacuum. The resulting bulk specimen was confirmed to be amorphous based on the X-ray diffraction patterns, as depicted in Fig. 1(a).

The germanium selenide film was fabricated using a thermal evaporation technique. Finely pulverized parent glass was thermally evaporated and deposited onto a (100) silicon wafer in a vacuum of better than  $2 \times 10^{-5}$  Torr. The surface areas of the GeSe<sub>2</sub> films were  $15 \times 15$  mm<sup>2</sup> and the thicknesses measured with an alpha step (KLA Tencor) were  $5.0 \pm 0.7$  μm. It is noteworthy that this thickness was achieved after ten repeated depositions under the abovementioned deposition conditions, and the atomic ratio of Ge to Se was experimentally confirmed to satisfy the stoichiometric Ge<sub>33</sub>Se<sub>67</sub> composition based on X-ray fluorescence spectrometry with a measurement uncertainty of  $\pm 1\%$ . Then, the film specimens were annealed at 320°C for 1 h in a vacuum. The X-ray diffraction patterns revealed that both the as-deposited and annealed GeSe<sub>2</sub> films were amorphous without noticeable crystalline phases, as depicted in Figs. 1(b) and 1(c), respectively.

The primary experiments to verify the feasibility of the imprinting technique used various static loads in the form of metallic lumps that were applied to a patterned Si stamp, which was placed in contact with the amorphous chalcogenide film. In addition to the static load, the temperature and duration were also carefully varied during each experiment. On the surface of the Si stamp, there were arrays of concave circles with different diameters ranging from 5 to 20 μm. We observed the morphological changes of the pressed surface using a scanning electron microscope equipped with an energy dispersive X-ray spectrometer (JSM-6701F, JEOL). The pressed film specimens were also subjected to X-ray inspection (Ultima IV, Rigaku). In addition, we measured the viscosity of the film specimen using a thermo-mechanical analyzer (TMA Q400, TA Instruments).

In parallel with the experiments on the surface defor-

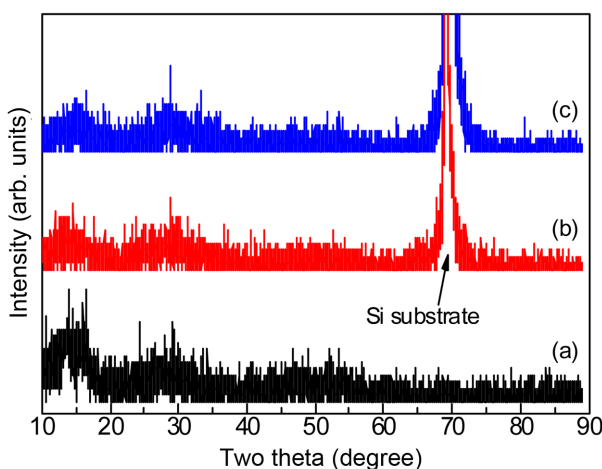


Fig. 1. X-ray diffraction pattern of (a) parent 'bulk' GeSe<sub>2</sub> glass and films (b) as-deposited and (c) annealed at 320°C for 1 h in a vacuum.

mation of the amorphous GeSe<sub>2</sub> film, we used extended X-ray absorption fine structure (EXAFS) spectroscopy to analyze the local structural environments of both constituent atoms before and after the crystallization. The amorphous GeSe<sub>2</sub> film specimen used in the EXAFS measurements was fabricated through thermally co-evaporating the elemental Ge and Se. These starting materials were deposited onto a 1 mm-thick SiO<sub>2</sub> glass substrate covered with 5 nm-thick ZnS SiO<sub>2</sub> layer, which was introduced for better adhesion. It should be noted that the vitreous silica functioned as a substrate, instead of the crystalline silicon wafer, in order to completely exclude the redundant Bragg peaks that resulted from the crystalline substrate during the EXAFS measurements in the fluorescence mode.<sup>7</sup> The prepared Ge-Se film was X-ray amorphous, and its composition was Ge<sub>30</sub>Se<sub>70</sub> (at%) with a measurement uncertainty of  $\pm 1.0$  at%. Its thickness was approximately 390 nm. In order to obtain annealed or partially crystallized specimens, some parts of the as-deposited amorphous film were heat-treated under an Ar atmosphere for 10 min at different temperatures, which were determined according to differential scanning calorimetric results.<sup>8</sup> In particular, two different temperatures were selected for the heat treatment: 340°C for relaxation and 420°C for partial crystallization. The X-ray absorptions at both the Ge K-edge and Se K-edge were measured in the fluorescence mode using the X18B beamline at the National Synchrotron Light Source, Brookhaven National Laboratory, USA. The procedures of the quantitative EXAFS analysis have been detailed in our previous reports.<sup>7,8</sup>

### 3. Results and Discussion

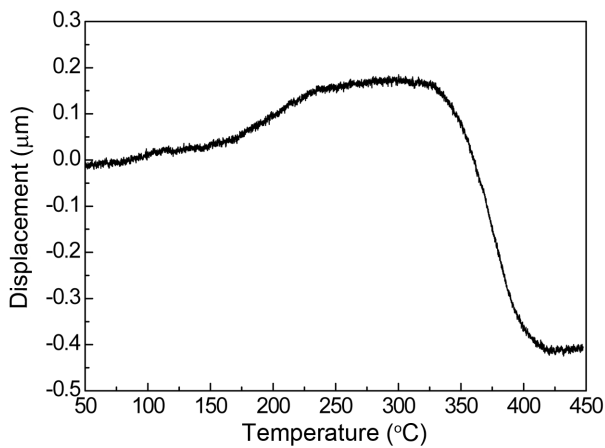
Regarding the imprinting conditions for amorphous chalcogenide films, temperature is a crucial processing parameter because an appropriate viscosity is required in order to guarantee a good imprinted surface that reflects the pattern (or shape) of the stamp. As such, the viscosity of our GeSe<sub>2</sub> film in the deformation range must be known. The viscosity of 'bulk' GeSe<sub>2</sub> glass at its glass transition temperature ( $\sim 300^\circ\text{C}$ ) is  $\sim 10^{13}$  poise, and it becomes  $\sim 10^{10}$  poise at  $370^\circ\text{C}$ ,<sup>9</sup> which is a good viscosity for the imprinting process. However, these viscosity values are not directly applicable to our film specimens, because the amorphous structures of the 'melt-quenched' bulk and 'vapor-quenched' film are not necessarily identical in most cases. For example, in the As<sub>2</sub>S<sub>3</sub> composition, homopolar bonds such as As-As and Se-Se are significantly more abundant in amorphous films rather than in bulk glasses.<sup>10</sup> Therefore, the viscosity ( $\eta$ ) of our film specimen was measured using the penetration method with the equation given below:<sup>11,12)</sup>

$$\eta = \frac{mMg}{8A^{0.5}\varepsilon}$$

Here,  $m$  is the geometrical coefficient of the probe ( $m = 0.96$  for cylindrical cross-section). The symbols  $M$ ,  $g$ , and  $A$

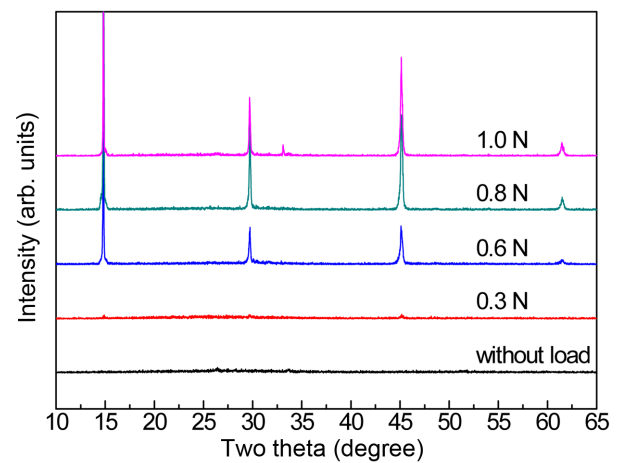
denote the load applied to the probe, the acceleration of gravity, and the area of the probe touching the sample surface, respectively. The penetration rate of the probe ( $\epsilon$ ) was obtained from the vertical displacement of the probe measured as a function of the temperature. In Fig. 2, it can be seen that a thermal expansion appears when the temperature is below  $\sim 300^\circ\text{C}$ , and then the probe penetration begins to occur above the softening point of the amorphous film. It was found that the temperature corresponding to a viscosity of  $10^{10}$  poise was approximately  $350^\circ\text{C}$ , which provides an initial starting point for the temperature in the imprinting experiments. In addition, in the previous studies,<sup>1-6)</sup> the processing temperatures were  $50 - 80^\circ\text{C}$  above the respective glass transition temperatures. Considering this, we initially set the temperature to  $350^\circ\text{C}$  in our experiments, which was then increased in  $10^\circ\text{C}$  increments to  $470^\circ\text{C}$ .

Figure 3 presents some representative surface morphologies of the film specimens that experienced different static loads at the same temperature of  $380^\circ\text{C}$ . Contrary to expectations, unfortunately, the patterns of the silicon stamp were not well resolved on the surface of the film specimens, but some irregularities that appear brighter were found instead. Here, the area of the brighter region that possibly originates from the surface crystallization increases with



**Fig. 2.** Displacement of the probe tip plotted as a function of the temperature. Note that a static load of 0.1 N is applied.

increases in the static load applied to the film surface. The X-ray diffraction patterns presented in Fig. 4 reveal some clear and sharp peaks that confirm almost invariably the existence of the monoclinic  $\text{GeSe}_2$  phase (JCPDS No. 71-0117). It is interesting to note that the intensity of the diffraction peaks tended to increase as the applied load increased. This behavior coincides well with what can be deduced from the morphological changes of the surface (see Fig. 3). As such, it can be considered that the present amorphous film tended to be crystallized when a mechanical load was applied statically, even though the processing temperature was sufficiently below the onset temperature of the crystallization. The silicon stamp that is in direct contact with the film would cause a new interface to develop that is likely to result in situations for heterogeneous nucleation. Nevertheless, it appears valid to presume that this amorphous  $\text{GeSe}_2$  film under the condition of constant loading is more vulnerable to surface crystallization than the amorphous  $\text{As}_2\text{Se}_3$  film under the same loading conditions. In an effort to verify whether or not any foreign particles function as sites for heterogeneous nucleation, we attempted to draw a two-dimensional map of the elemental distribution inside the pressed surface region using energy dispersive spectrometry. Fig. 5 presents a surface image in which the two



**Fig. 4.** X-ray diffraction patterns of the  $\text{GeSe}_2$  film specimens pressed with or without static loading. Note that the temperature and duration are fixed at  $380^\circ\text{C}$  and 10 min, respectively.

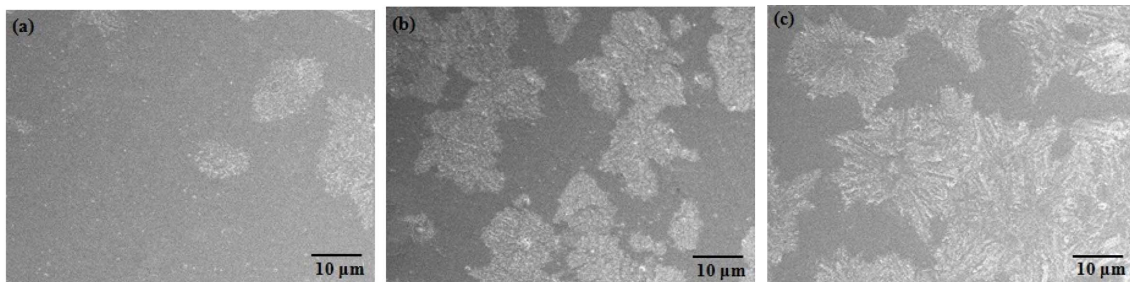


**Fig. 3.** Scanning electron microscopic images of the  $\text{GeSe}_2$  film pressed statically with (a) 0.3 N, (b) 0.6 N, and (c) 1.0 N. Note that all film specimens are pressed at  $380^\circ\text{C}$  for 10 min in a vacuum.

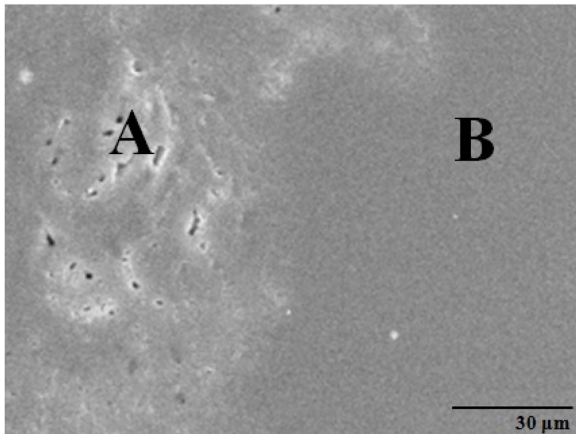


**Fig. 5.** Scanning electron microscopic image exhibiting a crystallized region marked with **A** and the remaining amorphous region **B** of the GeSe<sub>2</sub> film pressed with 0.8 N at 380°C for 10 min.

regions marked as **A** and **B** indicate the crystallized and amorphous regions, respectively. The results of the mapping indicate that foreign elements were not present other than Ge and Se, which maintained a ratio close to 33 : 67 across the area of the elemental distribution map. However, we attempted to further increase the processing temperature, even though a nontrivial amount of crystallization occurred in the surface. Fig. 6 illustrates one experiment conducted at higher temperatures; in this case, when the processing temperature was 470°C, the surface of the GeSe<sub>2</sub> film reflected the stamp patterns reasonably well.

The processing temperatures that have been reported previously for imprinting As-based chalcogenide films should be noted; for the As<sub>2</sub>S<sub>3</sub> film, the imprinting has been conducted at 255°C, which is ~70°C above its glass transition temperature and it provides a viscosity of ~10<sup>10</sup> poise.<sup>5,13</sup> For the As<sub>2</sub>Se<sub>3</sub> film, the processing temperature was 245°C, which was 75°C higher than its glass transition temperature, and its viscosity at this temperature was significantly lower than 10<sup>11</sup> poise.<sup>4,14</sup> These previous experimental results indicate that the suitable processing temperature for imprinting As-based binary glasses should be at least 70°C higher than their glass transition temperatures in order to secure an appropriate viscosity for mass flow. It is known that germanium-based binary chalcogenide glasses exhibit higher glass transition temperatures than arsenic-based counterparts.<sup>15-17</sup> In particular, the temperatures for the glass transition and crystallization of bulk GeSe<sub>2</sub> glass are ~300°C and ~420°C, respectively, whereas those of bulk As<sub>2</sub>Se<sub>3</sub> glass are ~170°C and ~300°C, respectively.<sup>18,19</sup> These values clearly indicate that the thermal stability of the GeSe<sub>2</sub> glass, given by the difference between the two temperatures, is significantly lower than As<sub>2</sub>Se<sub>3</sub> glass. Moreover, Ge-based binary glasses generally exhibit smaller activation energies for viscous flows compared with As-based binary glasses.<sup>4,9,14</sup> This implies that for the amorphous GeSe<sub>2</sub> film, it would be more difficult to establish

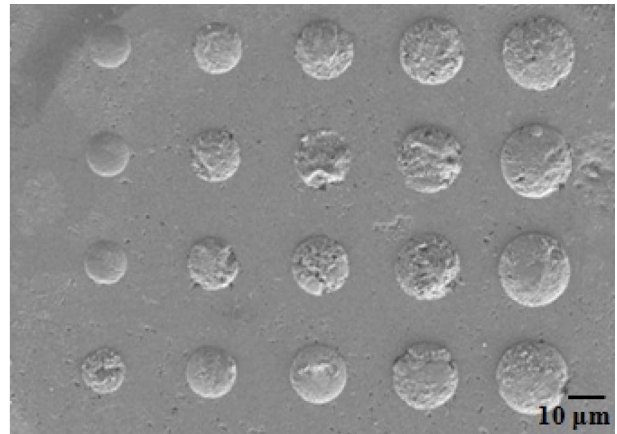


**Fig. 6.** Surface morphology of the GeSe<sub>2</sub> film deformed following the stamp patterns used in this study. A load of 1.0 N is statically applied at 470°C for 10 min in a vacuum.

appropriate imprinting conditions.

The facilitated surface crystallization observed from the GeSe<sub>2</sub> film under static loading conditions when compared with that of the As<sub>2</sub>Se<sub>3</sub> film could be explained in relation to its topological aspects, i.e. the connectivity of the constituent atoms in its amorphous structure. As is known, the amorphous structures of these Ge-Se and As-Se compositional systems satisfy the 8-*N* rule well.<sup>20-23</sup> Reflecting this empirical but powerful rule, the coordination numbers of Ge, As, and Se are 4, 3, and 2, respectively, for each glass forming region. Thus, the mean coordination number (MCN) for the Ge<sub>33</sub>Se<sub>67</sub> and As<sub>40</sub>Se<sub>60</sub> glasses was calculated to be 2.67 and 2.40, respectively. From the perspective of the topological model based on the constraints counting theory,<sup>24</sup> a glass structure becomes 'rigid' when the MCN is identical to or greater than 2.40. Thus, this reasoning implies that the amorphous structure of the Ge<sub>33</sub>Se<sub>67</sub> composition would be more rigid than that of the As<sub>40</sub>Se<sub>60</sub> composition, which partially supports the currently observed experimental result. Considering the dimensionality of both glass structures, it can be seen that the constituent atoms in the GeSe<sub>2</sub> film would be more connected with each other than those in the As<sub>2</sub>Se<sub>3</sub> film. More specifically, the dimensionality of the GeSe<sub>2</sub> film is closer to that of a three-dimensional network; thus, deformation under a static loading at elevated temperatures appears to be less probable in the GeSe<sub>2</sub> film.

Another aspect that should be considered is the relative fraction of the homopolar bonds in each glass structure. As is already known, homopolar bonds exist even in glass structures with these stoichiometric compositions. However, homopolar bonds such as As-As and Se-Se have been experimentally verified to be more abundant in As<sub>2</sub>Se<sub>3</sub> films than the Ge-Ge and Se-Se bonds in GeSe<sub>2</sub> films.<sup>10, 21</sup> It can be conjectured that the short-range structural units of the amorphous GeSe<sub>2</sub> film are likely to resemble those of the crystalline GeSe<sub>2</sub> compound significantly more when compared

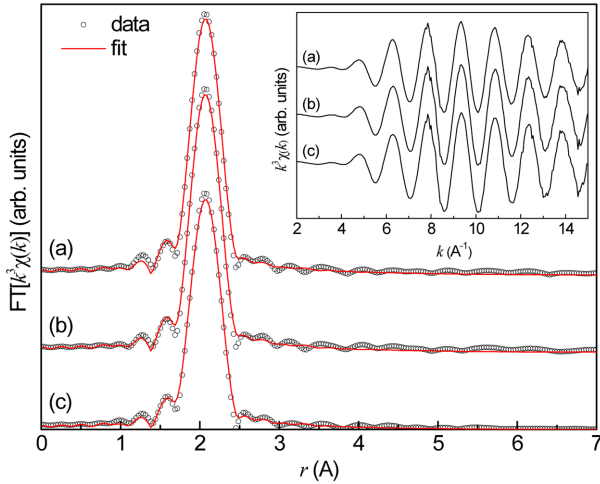


**Fig. 7.** The magnitude of the Fourier transform of the Ge K-edge EXAFS spectra of the  $\text{Ge}_{30}\text{Se}_{70}$  film (a) as-deposited and heat-treated at (b)  $340^\circ\text{C}$  and (c)  $420^\circ\text{C}$ . Note that the phase shifts are not corrected. The Fourier transform is performed in the photoelectron momentum ( $k$ ) range from 2.0 to  $15.0 \text{ \AA}^{-1}$  and the least-squares nonlinear fits are conducted in the  $R$  space ranging from 1.4 to  $3.0 \text{ \AA}$ . The inset displays the measured Ge K-edge EXAFS spectra plotted in the  $K$  space.

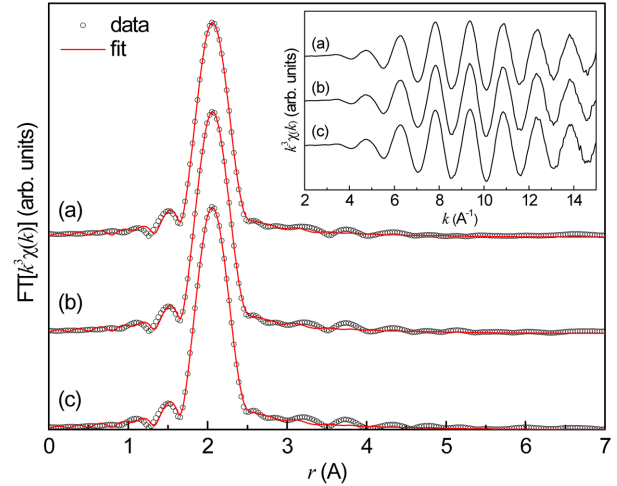


**Fig. 8.** The magnitude of the Fourier transform of the Se K-edge EXAFS spectra of the  $\text{Ge}_{30}\text{Se}_{70}$  film (a) as-deposited and heat-treated at (b)  $340^\circ\text{C}$  and (c)  $420^\circ\text{C}$ . The Fourier transform is performed in the  $k$  range from 2.0 to  $14.0 \text{ \AA}^{-1}$  and the least-squares nonlinear fits are conducted in the  $R$  space ranging from 1.4 to  $3.0 \text{ \AA}$ . The inset presents the measured Se K-edge EXAFS spectra plotted in the  $K$  space.

with that of the amorphous  $\text{As}_2\text{Se}_3$  film. Provided that the atomic arrangements in the tetrahedral  $[\text{GeSe}_{4/2}]$  unit of the amorphous  $\text{GeSe}_2$  film were reasonably close to those of its crystalline counterpart, the increased tendency of the surface crystallization would be supported from the structural viewpoint. It can be seen that the nearest neighboring peaks in the Ge K-edge EXAFS spectra of the  $\text{GeSe}_2$  film (Fig. 7) were almost identical to each other regardless of the annealing or crystallization. The local environments surrounding the Se atom were also preserved upon heat treatment without nontrivial changes as witnessed from the first coordination shell of the Se K-edge EXAFS spectra (Fig. 8). The results of our quantitative assessment using the EXAFS spectra of the  $\text{Ge}_{30}\text{Se}_{70}$  film primarily note that, as summarized in Table 1, only the Debye-Waller factors ( $\sigma^2$ ) for both Ge-Se and Se-Ge pairs tended to decrease after the crystallization occurred, whereas the coordination number ( $CN$ ) and inter-atomic distance ( $r$ ) of each atomic pair remained unchanged. Our EXAFS analyses indicate the close similarity of the  $[\text{GeSe}_{4/2}]$  units before and after crystallization. It has been reported that vitrification around this stoichiometric  $\text{GeSe}_2$  composition was most dif-

ficult, using the melt-quenching route, in the glass forming range of the binary Ge-Se system,<sup>25)</sup> which is in good agreement with the present EXAFS analyses. In addition, it is interesting to note that the first experimental demonstration of the chalcogenide glass formation was achieved using the stoichiometric  $\text{As}_2\text{S}_3$  composition,<sup>26)</sup> which partially supports the good thermal stability of the binary As-chalcogenide glasses.

#### 4. Conclusion

We prepared amorphous  $\text{GeSe}_2$  film using a thermal evaporation technique and investigated the changes in the surface morphology under various static loads applied at elevated temperatures. We found that the surface crystallization occurred relatively easily in the  $\text{GeSe}_2$  film compared with that in the  $\text{As}_2\text{Se}_3$  film. The amorphous structure of the  $\text{GeSe}_2$  film was significantly topologically constrained, and it possessed a relatively small amount of homopolar Ge-Ge and Se-Se bonds. In addition, the  $[\text{GeSe}_{4/2}]$  unit in its amorphous phase was similar to that of its crystalline phase. As a result of these attributes, the amorphous state appeared to be more vulnerable to crystallization during the thermo-

**Table 1.** Structural Parameters Optimized from the EXAFS Spectroscopic Analyses

	Ge-Se pair				Se-Ge pair			
	$CN$	$r$ (Å)	$\sigma^2$ ( $\times 10^{-4} \text{ \AA}^2$ )	$R$ -factor ( $\times 10^{-5}$ )	$CN$	$r$ (Å)	$\sigma^2$ ( $\times 10^{-4} \text{ \AA}^2$ )	$R$ -factor ( $\times 10^{-5}$ )
as-deposited	$3.8 \pm 0.2$	$2.36 \pm 0.01$	$40 \pm 3$	1.7	$2.0 \pm 0.2$	$2.36 \pm 0.01$	$36 \pm 2$	0.2
heat-treated at $340^\circ\text{C}$	$4.0 \pm 0.2$	$2.36 \pm 0.01$	$37 \pm 3$	1.1	$2.0 \pm 0.2$	$2.36 \pm 0.01$	$35 \pm 2$	0.8
heat-treated at $420^\circ\text{C}$	$3.9 \pm 0.2$	$2.36 \pm 0.01$	$37 \pm 3$	0.6	$2.0 \pm 0.2$	$2.36 \pm 0.01$	$34 \pm 2$	0.3

mechanical deformation. This study exemplifies the effects of the glass structures on the imprinting process; because Ge-based chalcogenide glasses are normally more recommended for practical applications than As-based ones, Se-sufficient Ge-Se compositions, which have smaller MCNs than the stoichiometric GeSe<sub>2</sub> composition, are preferable in order to retard unwanted surface crystallization during the imprinting process.

### Acknowledgments

YGC is grateful to Dr. B. K. Cheong and Prof. H. Jain for the preparation of the EXAFS specimens and arrangement of the beamtime for the EXAFS measurements, respectively. This work was supported by the Basic Science Research Program of the National Research Foundation of Korea (NRF) funded by the Ministry of Education, Science and Technology (2012R1A1A2003832).

### REFERENCES

1. A. B. Seddon, W. J. Pan, D. Furniss, C. A. Miller, H. Rowe, D. Zhang, E. M. Brearty, Y. Zhang, A. Loni, P. Sewell, and T. M. Benson, "Fine Embossing of Chalcogenide Glasses – A New Fabrication Route for Photonic Integrated Circuits," *J. Non-Cryst. Solids*, **352** [23-25] 2515-20 (2006).
2. W. J. Pan, D. Furniss, H. Rowe, C. A. Miller, A. Loni, P. Sewell, T. M. Benson, and A. B. Seddon, "Fine Embossing of Chalcogenide Glasses: First Time Submicron Definition of Surface Embossed Features," *J. Non-Cryst. Solids*, **353** [13-15] 1302-06 (2007).
3. W. J. Pan, H. Rowe, D. Zhang, Y. Zhang, A. Loni, D. Furniss, P. Sewell, T. M. Benson, and A. B. Seddon, "One-Step Hot Embossing of Optical Rib Waveguides in Chalcogenide Glasses," *Microw. Opt. Tech. Lett.*, **50** [7] 1961-63 (2008).
4. Z. G. Lian, W. Pan, D. Furniss, T. M. Benson, A. B. Seddon, T. Kohoutek, J. Orava, and T. Wagner, "Embossing of Chalcogenide Glasses: Monomode Rib Optical Waveguides in Evaporated Thin Films," *Opt. Lett.*, **34** [8] 1234-36 (2009).
5. M. Solmaz, H. Park, C. K. Madsen, and X. Cheng, "Patterning Chalcogenide Glass by Direct Resist-Free Thermal Nanoimprint," *J. Vac. Sci. Tech. B*, **26** [2] 606-10 (2008).
6. T. Han, S. Madden, D. Bulla, and B. L. Davies, "Low Loss Chalcogenide Glass Waveguides by Thermal Nano-Imprint Lithography," *Opt. Express*, **18** [18] 19286-91 (2010).
7. Y. G. Choi, A. Kovalskiy, B. K. Cheong, and H. Jain, "Role of Local Structure in the Phase Change of Ge-Te Films," *Chem. Phys. Lett.*, **534** 58-61 (2012).
8. Y. G. Choi, S. Y. Shin, R. Golovchak, S. Lee, B. K. Cheong, and H. Jain, "EXAFS Spectroscopic Refinement of Amorphous Structures of Evaporation-Deposited Ge-Se Films," *J. Alloys Compd.*, **622** 189-93 (2015).
9. U. Senapati and A. K. Varshneya, "Viscosity of Chalcogenide Glass-Forming Liquids: An Anomaly in the 'Strong' and 'Fragile' Classification," *J. Non-Cryst. Solids*, **197** [2-3] 210-18 (1996).
10. H. Jain, A. Kovalskiy, and A. Miller, "An XPS Study of the Early Stages of Silver Photodiffusion in Ag/a-As<sub>2</sub>S<sub>3</sub> Films," *J. Non-Cryst. Solids*, **352** [6-7] 562-66 (2006).
11. W. J. Chung, H. S. Seo, B. J. Park, J. T. Ahn, and Y. G. Choi, "Selenide Glass Optical Fiber Doped with Pr<sup>3+</sup> for U-Band Optical Amplifier," *ETRI J.*, **27** [4] 411-17 (2005).
12. C. J. Hill, L. Huang, and A. Jha, "High-Tg GeS<sub>2</sub> Based Glasses for Chemical Sensing Applications," *J. Mater. Sci. Mater. El.*, **20** [1] S202-06 (2009).
13. J. Malek, "Dilatometric Study of Structural Relaxation in Arsenic Sulfide Glass," *Thermochim. Acta*, **311** [1-2] 183-98 (1998).
14. S. Suzuki, T. Kobayashi, H. Ohno, and S. Kamiya, "Viscosity of Glasses in the System As-Se and As-Se-X (X=I, S) in the Transition Region," *J. Soc. Mater. Sci. Jpn.*, **22** 134-39 (1973).
15. S. M. Song and S. Y. Choi, "Preparation and Characterization of Chalcogenide Glass with IR-Transmittance (*In Korean*)," *J. Korean Ceram. Soc.*, **32** [12] 1424-32 (1995).
16. J. A. Savage, P. J. Webber, and A. M. Pitt, "An Assessment of Ge-Sb-Se Glasses as 8 to 12 mm Infrared Optical Materials," *J. Mater. Sci.*, **13** [4] 859-64 (1978).
17. K. N. Madhusoodanan and J. Philip, "Thermal Diffusion near Glass Transition in Ge-Se Glasses Measured by Photoacoustics," *Pramana - J. Phys.*, **32** [6] 821-30 (1989).
18. D. Lezal, J. Zavadil, and M. Prochazka, "Sulfide, Selenide and Telluride Glassy Systems for Optoelectronic Applications," *J. Optoelectron. Adv. Mater.*, **7** [5] 2281-92 (2005).
19. V. V. Tomaev, Y. S. Tver'yanovich, M. D. Bal'makov, I. A. Zvereva, and A. B. Missyul, "Ionic Conductivity of (As<sub>2</sub>Se<sub>3</sub>)<sub>1-x</sub>(AgHal)<sub>x</sub> (Hal = I, Br) Nanocomposites," *Glass Phys. Chem.*, **36** [4] 455-62 (2010).
20. V. Petkov, D. Qadir, and S. D. Shastri, "Rapid Structure Determination of Disordered Materials: Study of GeSe<sub>2</sub> Glass," *Solid State Commun.*, **129** [4] 239-43 (2004).
21. I. Petri and P. S. Salmon, "Defects in a Disordered World: The Structure of Glassy GeSe<sub>2</sub>," *Phys. Rev. Lett.*, **84** [11] 2413-16 (2000).
22. J. C. Mauro and A. K. Varshneya, "Multiscale Modeling of Arsenic Selenide Glass," *J. Non-Cryst. Solids*, **353** [13-15] 1226-31 (2007).
23. M. Fabian, E. Svab, V. Pamukchieva, A. Szekeres, S. Vogel, and U. Ruett, "Study of As<sub>2</sub>Se<sub>3</sub> and As<sub>2</sub>Se<sub>2</sub>Te Glass Structure by Neutron- and X-ray Diffraction Methods," *J. Phys. Conf. Ser.*, **253** [1] 012053 (2010).
24. J. C. Phillips, "Topology of Covalent Non-Crystalline Solids I: Short-Range Order in Chalcogenide Alloys," *J. Non-Cryst. Solids*, **34** [2] 153-81 (1979).
25. R. Azoulay, H. Thibierge, and A. Brenac, "Devitrification Characteristics of Ge<sub>x</sub>Se<sub>1-x</sub> Glasses," *J. Non-Cryst. Solids*, **18** [1] 33-53 (1975).
26. R. Frerichs, "New Optical Glasses Transparent in Infrared up to 12 μm," *Phys. Rev.*, **78** 643 (1950).